

Short Communication

Aptamer based rGO-AuNPs Electrochemical Sensors and its Application for Detection of *Salmonella Anatum* in Food

Mingyan Chai

Department of Pharmacy and Biotechnology, Zibo Vocational Institute, Zibo 255314, China
E-mail: mingyan_chai@163.com

Received: 3 Sepyember 2021 / Accepted: 29 October 2021 / Published: 6 December 2021

Foodborne pathogenic bacteria can cause food poisoning or infection. *Salmonella* is an aerobic or partly anaerobic gram-negative bacterium that enters the body with food, invades the intestine and releases large amounts of endotoxin. The endotoxin acts as a pyrogen that leads to an increase in body temperature and acts on the intestinal mucosa to trigger systemic inflammation and toxic symptoms in the host. The development of novel methods and systems for the monitoring and detection of foodborne pathogenic bacteria is of great significance for food safety, especially the development of simple, high-throughput and highly sensitive rapid detection techniques. This work proposes a novel aptamer sensor based on reduced graphene oxide (rGO)-AuNPs for the detection of *Salmonella* in food. Firstly the rGO and AuNPs were modified on the surface of glassy carbon electrode in turn, and then a highly sensitive sensor was made by designing a segment of thiolated aptamer probe that could specifically capture *Salmonella*. The high electron transport ability of rGO and the advantage of large specific surface area of AuNPs were adopted to achieve signal amplification and improve the detection capability. In the presence of *Salmonella*, the aptamer traps and immobilizes *Salmonella* on the surface of the electrode, resulting in a change in the immediate current in the sensor and realizing quantitative detection of *Salmonella* based on the change in electrical signal. Under the optimized conditions, the response current of the constructed aptamer sensor is linearly related to the logarithmic value of *Salmonella* concentration, with a linear range of 6×10^2 cfu/mL~ 6×10^7 cfu/mL and a detection limit of 200 cfu/mL (S/N=3). Meanwhile, this sensor has been successfully applied in the detection of *Salmonella* in pork and beef.

Keywords: Foodborne pathogenic bacteria; Aptamer sensor; Reduced graphene oxide; Electrochemical impedance; Label-free detection

1. INTRODUCTION

Salmonella infection has been a long-term concern in public health safety. Foodborne illnesses caused by *Salmonella* accounts for 11.66% of the total foodborne illness outbreaks and is the third

leading causative agent of foodborne illnesses [1–3]. *Salmonella* is continuously threatening people's life and health, therefore, it is of great importance for the detection of *Salmonella* in food [4–9].

Salmonella is a gram-negative bacillus with more than 2650 serotypes [10], among which *Salmonella typhimurium* and *Salmonella paratyphi* A are susceptible to enteric fever. *Salmonella typhimurium* serotype is the most predominant *Salmonella* that can cause systemic infection [11]. Biosensors are a class of devices that combine biological signals with physical or chemical transducers and transform them into signals that can be monitored [12], and they have gradually gained a widespread application because of their excellent performance in *Salmonella* detection. Among the various types of sensors, nanomaterial-based biosensors are the best performing biosensors available [13–18]. The use of biosensors is easier and timesaving, which is conducive to the real time detection of *Salmonella* in the field [19–23].

The traditional techniques for the detection of *Salmonella* mainly include conventional culture methods, nucleic acid analysis, immunological assays, etc. The conventional culture method is based on various industry standards and national standards, which are highly reliable, but there are some limitations in this method [24–30]. The antigenicity of the same serotype of *Salmonella* may be different due to the alteration or loss of surface antigens, resulting in a low sensitivity of serological detection methods, which can easily produce false negatives [31,32]. In addition, there is much crossover in biochemical reactions among Enterobacteriaceae, which may result in false positives [33]. Nucleic acid analysis is a technique for amplification or identification of nucleic acid sequences specific for *Salmonella* [34], for *Salmonella* contains a specific invasion protein A (invA) gene [35]. This fragment designed primers and probes for polymerase chain Reaction (PCR) identification is a common method for *Salmonella* detection in the laboratory. The nucleic acid analysis method that has been adopted currently has high specificity and accuracy, but requires specialized instrumentation and good staff practice, being not able to meet the requirements for rapid detection in large-scale outbreaks of *Salmonella* infection [36]. Immunological assays rely on the specific binding of antigenic antibodies to amplify the biological signal into a chemical signal that can be monitored for the detection of bacteria [37]. Compared with the conventional culture methods, immunological assays are highly specific and sensitive, and are commonly used in pathogenic bacteria detection. However, all these methods have some potential drawbacks in *Salmonella* detection, such as the consumption of time and the presence of cross-reactivity [38].

Biosensor detection of *Salmonella* is based on specific recognition of antigen antibody, as well as nucleic acid or aptamer specific recognition of the bacterium [39]. It amplifies and converts the biological signal into an optical or electrochemical signal to achieve detection by establishing a relationship between the chemical signal and the concentration of *Salmonella* [40]. Current-based biosensor is a detection technology based on the change of current as a sign of biosignal amplification, converting the biosignal into a current signal by generating a change in the electrical properties of the ionic polymer through the biosignal or a change in the electrode surface current through electron transfer. Several current-based biosensors have been applied for *Salmonella* detection. Silva et al [41] coated AuNPs polymeric envelope on the surface of a homemade electrode as an element for output signal amplification and as a curing platform for antibodies based on the principle that polymeric ion-selective electrodes are highly sensitive to changes in zero-current ion flow. Before the binding of *Salmonella*,

the ion influx in the electrode inner filling reaches a steady state, while after the addition of *Salmonella*, the immobilized antibody on the sensor surface binds to *Salmonella* leading to a blocking effect of ion flux, which results in a potential shift, and *Salmonella typhimurium* in the sample can be detected by the amount of potential shift. This method is sensitive and easy to use with a short detection time, however, it cannot be adopted for quantitative detection of *Salmonella spp.* Rao et al [42] applied recombinant DNA recombinant technology in the preparation of recombinant flagellar fusion protein-wrapped screen-printed electrodes to form a flagellar fusion protein-serum *Salmonella*-phosphatase-labeled antibody detection platform. 1-naphthol produced by alkaline phosphatase hydrolysis is used in this method as the detection signal for the amperometric assay, which can sensitively detect *Salmonella* in human serum and form a clear control of the detection results of healthy human serum. In addition, the oxidative reduction of H₂O₂ by hydroquinone in the presence of horseradish peroxidase can cause a decrease in the peak current.

This work establishes an aptamer sensor based on rGO-AuNPs, adopts an improved method to produce a stable graphene oxide (GO) and explores the electrochemical reduction of GO. The nanomaterials were characterized by scanning electron microscopy and the working electrode assembly steps were characterized by cyclic voltammetry and electrochemical impedance methods. An aptamer sensor for the direct detection of *Salmonella* (ATCC 9270) was developed by adding a whole bacteria capture probe of *Salmonella* and optimizing the incubation time and other parameters. Finally, the method was validated in real samples with spiked recovery.

2. EXPERIMENTAL

2.1 Materials

The *Salmonella* aptamer was synthesized by Shanghai Bioengineering Biotechnology Service Co., LTD. and diluted with TE buffer (10 mM Tris-HCl, 1 mM EDTA, pH=7.5) and stored frozen at -20°C when not in use.

Sequence: 5'-HS-(CH₂)₆-TAT GGC GGC GTC ACC CGA CGG GGA CTT GAC ATT ATG ACA-G-3';

Chloroauric acid was purchased from Aladdin Reagent Co. Yeast extract and tryptone were purchased from Shanghai Ye Yuan Biological Preparation Co. Disodium hydrogen phosphate, sodium nitrate, sodium dihydrogen phosphate, potassium ferricyanide, potassium ferrocyanide, potassium chloride, sodium hydroxide, potassium permanganate, potassium dihydrogen phosphate, hydrogen peroxide, sodium chloride, tris(hydroxymethyl)aminomethane (Tris), concentrated sulfuric acid, anhydrous ethanol, 2-mercaptoethanol and solid agar were purchased from Sinopharm Chemical Reagent Co. The experimental water was Milipore ultrapure water ($\geq 18 \text{ M}\Omega/\text{cm}$). *Salmonella Anatum* (ATCC 9270) was purchased from BNA Chuanglian Biotechnology Co., LTD.

Pork and beef were purchased from local supermarket.

2.2 Preparation of graphene oxide

GO was prepared by the conventional Hummers method [43,44]. Specifically, 2.0 g of graphite flakes and 1.6 g of sodium nitrate were added sequentially to a volume of 67.5 mL of 98% H₂SO₄, and the conditions were maintained in an ice bath. Afterwards, 9.0 g of potassium permanganate was added and stirred for 30 min with magnetic stirrer, and the reaction was kept at room temperature for 5 days. After 560 mL of ultrapure water was slowly added to the reactor, the suspension was treated with 30% hydrogen peroxide solution until it turned bright yellow. Finally, the suspension was centrifuged, washed and dried to obtain GO.

2.3 Assembly of electrochemical aptamer sensors

0.5 mg of the prepared GO was precisely weighed and dissolved in 1 mL of PBS buffer, and was sonicated for 30 min to obtain a homogeneous and stable solution. A certain amount of GO suspension was applied to the surface of the bare glassy carbon electrode (GCE) and dried naturally at room temperature (denoted as GO/GCE), after which the GO was reduced to rGO by electrochemical reduction in 0.1 M PBS reduction solution with cyclic voltammetry. The working conditions were as follows: working voltage of -0.2 V to 1.0 V, scan rate of 100 mV/s, and number of cycles of 50 (denoted as rGO/GCE). The deposition was performed in 1% chloroauric acid with amperometry deposition. The working conditions were as follows: the working voltage was -300 mV and the working time was 30 s. After the electrode was dried, 5 μ L of *Salmonella* aptamer was applied dropwise to the electrode surface and dried. Finally, the electrode was closed with 2-mercaptoethanol at a concentration of 0.1 M for 0.5 h to obtain an electrode with a *Salmonella* capture probe immobilized on the surface (denoted as rGO-AuNP).

2.4 Activated culture and enumeration of *Salmonella*

The original *Salmonella* strain was inoculated into LB liquid medium under aseptic conditions and incubated at 37°C for 12 h to activate and proliferate the bacteria. 25 mL of *Salmonella* sample was aspirated into a sterile conical flask with 225 mL of physiological saline and shake it thoroughly to make original *Salmonella* bacterial solution. Under aseptic conditions, 100 μ L of the original bacterial solution was slowly injected into a sterilized centrifuge tube containing 900 μ L of sterilized saline and shaken to mix thoroughly to make a 1:10 sample solution. Three different concentrations of 10⁻⁵~10⁻⁷ were selected for counting, 100 μ L of *Salmonella* solution was injected into LB solid plate medium and three plates were coated in parallel for each concentration. The plates were incubated at 37°C, observed and counted, and the number of dilutions and the corresponding number of colonies were recorded.

2.5 Electrochemical characterization and measurement

Cyclic voltammetry and electrochemical impedance methods were applied in electrochemical characterization and measurement. The cyclic voltammetry conditions were as follows: scanning voltage

of -0.2 V~0.6 V, and scan rate of 50 mV/s. The cyclic voltammograms of the bare electrode and the GO, rGO and rGO-AuNPs modified glassy carbon electrodes were obtained by subjecting the modified electrodes of different assembly steps to cyclic voltammetry in potassium ferrocyanide electrolyte. The electrochemical impedance conditions were as follows: the applied voltage was 0.2 V, the frequency range was 10^5 Hz~0.1 Hz, and the amplitude was 2 mV, with which the electrochemical impedance plots were obtained for the bare electrode and the GO, rGO, and rGO-AuNPs modified glassy carbon electrodes.

Salmonella solutions were diluted sequentially to 8 concentration gradients with sterilized saline for a test. The working electrode of the prepared modified capture probe was incubated with the bacterial solution diluted to 10^8 concentrations at a constant temperature of 37°C for 35 min and then measured by cyclic voltammetry in an electrochemical workstation. Under the same conditions, cyclic voltammetry curves were measured sequentially in different concentration gradients of the bacterial broth.

2.6 Meat sample processing

Pork and beef were used as actual samples for spiked recovery experiments. The meat samples were first surface sterilized, and 25 g of deep muscle was cut and shredded under aseptic conditions, and carefully ground with sterilized sand, after which 225 mL of sterilized water was added, shaken and mixed to produce a 1:10 dilution. Subsequently, different concentrations of *Salmonella* were added, mixed and tested by the above method, and the results were compared with those of plate counting to obtain the recovery rate.

3. RESULTS AND DISCUSSION

Figure 1 shows the preparation process of the *Salmonella* aptamer sensor constructed in this work. Firstly, the GO was modified on the surface of the bare GCE and dried naturally. The GO was reduced to rGO by electrochemical reduction in PBS solution. The oxygen-containing hetero-functional groups of GO were removed with the reduction process, thus the structure and properties of rGO could be closer to those of graphene and its electron transport properties were greatly enhanced [45]. A layer of AuNPs was subsequently immobilized on the electrode surface by electrochemical deposition. The good biocompatibility of AuNPs facilitated the immobilization of the aptamer, and the excellent electron transport ability also helped to improve the electron transport, while the large specific surface area can immobilize more capture probes. Finally, the sulfhydrylated *Salmonella* aptamer was added and firmly fixed on the surface of the AuNPs modified electrode through gold-sulfur bonds to build a working electrode [46,47]. During *Salmonella* detection, the aptamer can specifically trap *Salmonella* on the surface of the constructed working electrode, causing a change in electrochemical signal and a decrease in the immediate current value. Since the change of peak current value is linearly related to the

concentration of *Salmonella* within a certain range, this study has achieved the quantitative detection of *Salmonella* by measuring the change of peak current before and after capturing *Salmonella*.

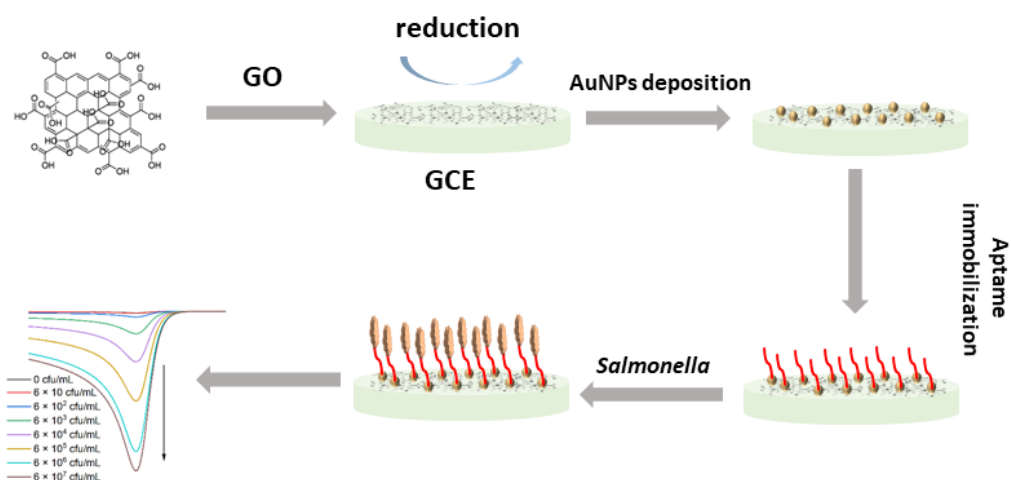


Figure 1. Schematic representation of the GCE surface modification and the detection of *Salmonella*.

The electrochemical impedance (EIS) and CV methods were adopted to examine the sensors constructed in this study to complete the verification of the electrode modifications at each step. As shown in the cyclic voltammetry curve of the bare electrode (Figure 2A), the peak current is much higher than that of the graphene oxide modified GCE, the reason for which is that the GO surface contains a large number of epoxy groups and other oxygen-containing hetero-functional groups, which occupy the electroactive sites on the electrode surface and block the electron transfer, leading to the decrease of peak current and the increase of resistance [48,49]. When GO is electrochemically reduced to rGO, the oxygen-containing hetero-functional groups of GO are removed by reduction, resulting in a graphene-like structure and function of rGO, with a significantly higher electron transfer capability [50]. Graphene has good electrical conductivity and electrocatalytic activity, and has been widely used in the field of biosensing [51]. From the figure it can be seen that the peak current value of the rGO is significantly higher than that of the normal GO, which also proves the successful reduction of GO. After the final modification with AuNPs by electrodeposition, the peak current value increases sharply. The reason for this phenomenon is that nanogold has high electron density and strong catalytic activity. Moreover, the large specific surface area and high surface free energy of nanogold particles can be used in biosensors to increase the capture probe loading, thus the signal amplification can be enhanced [52].

For EIS, $[\text{Fe}(\text{CN})_6]^{4-/3-}$ coupling is used as a redox probe and the resistance (R_{ct}) to charge transfer is determined by the impedance profile. Figure 2B shows that the resistance value of the bare electrode is about 1640 Ω . When the electrode is modified with GO, it affects the electron transfer, resulting in a decrease in current and an increase in resistance to 3.23 k Ω . The rGO after reduction significantly improves the electron transfer and reduces the resistance to 2.11 k Ω . After deposition of AuNPs, the resistance is as low as about 667 Ω , indicating that the introduction of AuNPs greatly enhances the electron transfer capability and successfully achieves signal amplification [53]. The EIS and CV

characterization yielded consistent results, jointly demonstrating the successful assembly of the electrodes.

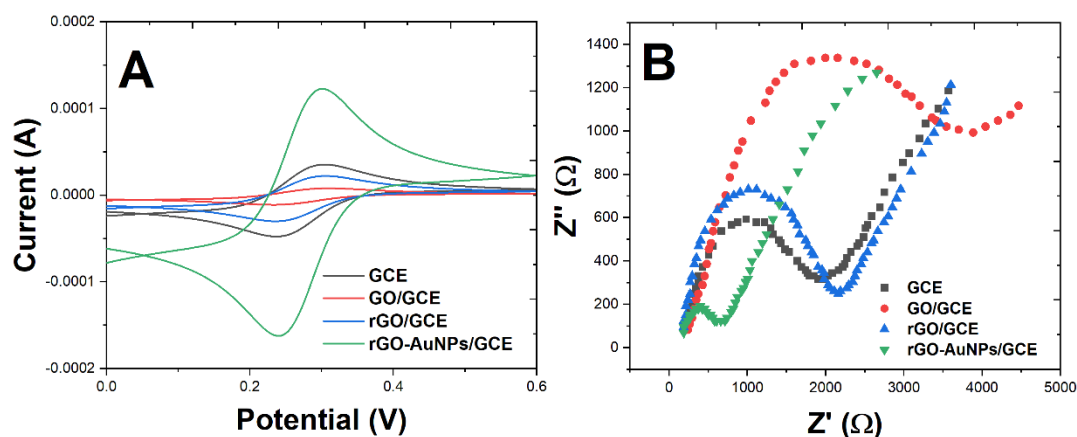


Figure 2. (A) CVs and (B) EIS plots of bare GCE, GO/GCE, rGO/GCE and rGO-AuNPs/GCE in 0.1 M KCl solution containing 5 mM $K_3[Fe(CN)_6]/K_4[Fe(CN)_6]$ (pH 7.4).

The characterization of GO modified on the surface of GCE by electrochemical reduction is shown in Figure 3A, from which it can be clearly seen that the electrode surface is a thin layer of graphene-like folded structure [54].

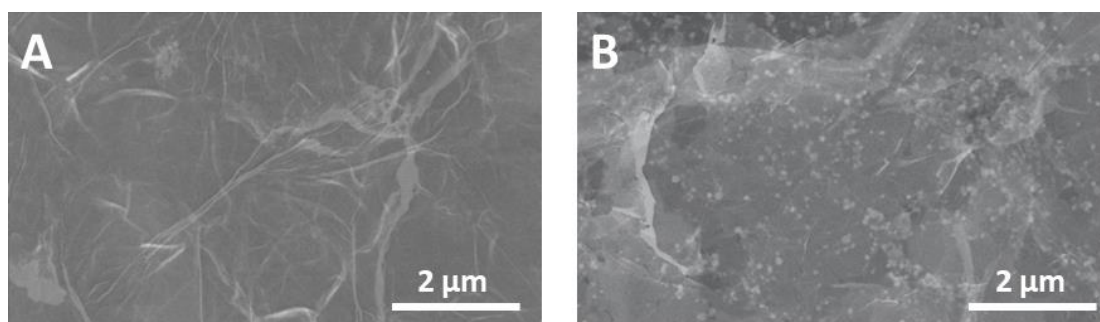


Figure 3. SEM image of (A) rGO/GCE and (B) rGO-AuNPs/GCE.

Figure 3B presents the SEM image of rGO-AuNPs/GCE. It can be noted that the AuNPs are successfully modified on the surface of the rGO material with uniform particle size and distribution. The introduction of AuNPs improves the specific surface area of the electrode, which can help to load more trapping probes.

The incubation time of the working electrode in *Salmonella* broth needs to be optimized. The electrode was incubated in *Salmonella* solution at 37°C with a dilution gradient of 10^{-6} . The time unit for aptamer capture was set to 5 min, and the CV and peak current change values were measured every 5 min. As the incubation time increases, the intensity and quantity of aptamer binding to *Salmonella* increase. The number of captured *Salmonellae* increases while the peak current values decrease

significantly[55]. If the incubation time is too short, the aptamer will not bind to *Salmonella* completely and the results will not be stable. However, it is not able to meet the requirements for rapid food safety testing with an excessively long time.

The performance of the electrochemical aptamer sensor constructed in this experiment was investigated under the optimal experimental conditions for the detection of *Salmonella*. Figure 4A shows the differential pulse voltammetry (DPV) curves obtained by incubating the sensor electrode in different concentrations of *Salmonella* for 30 min, including the blank control and different dilution gradients of *Salmonella*. When the concentration of the bacterial solution increases, the peak current also increases gradually. At the concentration of the bacterial solution of 6×10^2 - 6×10^7 cfu/mL, the difference of the peak current of DPV maintains a good linear relationship with the logarithm of the bacterial solution concentration, and the detection limit is 200 cfu/mL (S/N=3) (Figure 4B). The detection of *Salmonella* can be achieved within 1 h with this method which is simpler, more economical and efficient than the traditional isolation and culture method (Table 1).

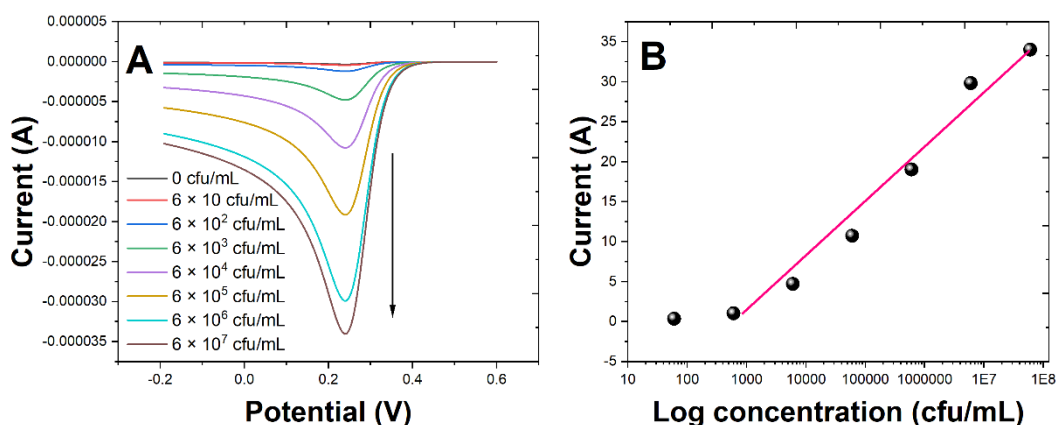
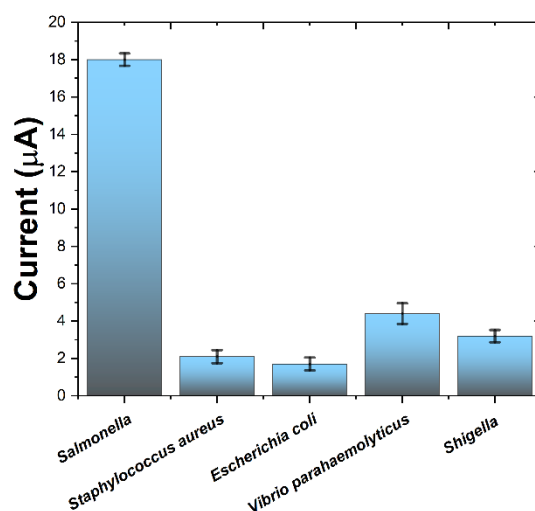


Figure 4. (A) DPV curves obtained when detecting *Salmonella* in different concentrations (0 - 6×10^7 cfu/mL). (B) Calibration curve of concentrations of *Salmonella* against the current value.

In this experiment, the selectivity of the *Salmonella* aptamer sensor was investigated by using the common foodstuffs *Staphylococcus aureus*, *Escherichia coli*, *Vibrio parahaemolyticus* and *Shigella* as control experiments. Under the optimal experimental conditions, the working electrodes were incubated with different strains for 30 min, and the changes in peak current values were measured. As shown in Figure 5, a much larger decrease in peak current value was caused by *Salmonella* than other strains, indicating that the aptamer designed in this experiment has high specificity for the detection of *Salmonella*.

Table 1. Performance compared with other reported aptasensors for *Salmonella* detection.

Method	Linear range (cfu/mL)	LOD (cfu/mL)	Reference
Electrochemical immunosensor	1×10^2 to 1×10^6	1×10^2	[56]
MRS immunosensor	1×10^3 to 1×10^6	1×10^3	[57]
Electrochemical immunosensor	1×10^3 to 1×10^7	5×10^2	[58]
Electrochemical immunosensor	1×10^3 to 1×10^6	1×10^3	[59]
Electrochemical aptasensor	1×10^3 to 1×10^8	1×10^2	[60]
Electrochemical aptasensor	6×10^2 to 6×10^7	2×10^2	This work

**Figure 5.** The selectivity of the proposed aptasensor.

Pork and beef samples with different concentrations of *Salmonella* were tested with the aptamer sensor designed in this experiment and the recovery was calculated with the plate count method for comparison. Table 2 reveals that the results of this method are consistent with those of the plate counting method with the recoveries ranging from 97.13% to 107.70%, which indicates that the aptamer sensor designed in this experiment is highly accurate for the detection of *Salmonella* and can be used for actual sample detection.

Table 2. The recovery of *Salmonella* detection in pork and beef samples.

Sample	Found (cfu/mL)	Added (cfu/mL)	Found (cfu/mL)	Recovery (%)	RSD (%)
Pork 1	0	1500	1457	97.13	3.11
Pork 2	0	3000	3204	106.80	2.59
Beef 1	0	10000	10770	107.70	6.03
Beef 2	0	50000	48711	97.42	3.57

4. CONCLUSION

In conclusion, a novel aptamer sensor based on rGO-AuNPs was prepared for the detection of *Salmonella* in food in this study. rGO and AuNPs were successively modified on the surface of GCE, and a highly sensitive sensor was fabricated by designing a segment of thiolated aptamer probe that could specifically capture *Salmonella*. Under the optimized conditions, the constructed aptamer sensor response current is linearly related to the logarithmic value of *Salmonella* concentration with a linear range of 6×10^2 cfu/mL \sim 6×10^7 cfu/mL and a detection limit of 200 cfu/mL (S/N=3). Moreover, the sensor can be applied to actual samples and has good selectivity.

References

1. J.N. Appaturi, T. Pulingam, K.L. Thong, S. Muniandy, N. Ahmad, B.F. Leo, *Anal. Biochem.*, 589 (2020) 113489.
2. S. Muniandy, S.J. Teh, J.N. Appaturi, K.L. Thong, C.W. Lai, F. Ibrahim, B.F. Leo, *Bioelectrochemistry*, 127 (2019) 136–144.
3. H. Karimi-Maleh, Y. Orooji, F. Karimi, M. Alizadeh, M. Baghayeri, J. Rouhi, S. Tajik, H. Beitollahi, S. Agarwal, V.K. Gupta, *Biosens. Bioelectron.* (2021) 113252.
4. P. Murasova, A. Kovarova, J. Kasparova, I. Brozkova, A. Hamiot, J. Pekarkova, B. Dupuy, J. Drbohlavova, Z. Bilkova, L. Korecka, *J. Electroanal. Chem.*, 863 (2020) 114051.
5. R. Duan, X. Fang, D. Wang, *Front. Chem.*, 9 (2021) 361.
6. C. Li, F. Sun, *Front. Chem.*, 9 (2021) 409.
7. H. Karimi-Maleh, M. Alizadeh, Y. Orooji, F. Karimi, M. Baghayeri, J. Rouhi, S. Tajik, H. Beitollahi, S. Agarwal, V.K. Gupta, S. Rajendran, S. Rostamnia, L. Fu, F. Saberi-Movahed, S. Malekmohammadi, *Ind. Eng. Chem. Res.*, 60 (2021) 816–823.
8. L. Fu, K. Xie, A. Wang, F. Lyu, J. Ge, L. Zhang, H. Zhang, W. Su, Y.-L. Hou, C. Zhou, C. Wang, S. Ruan, *Anal. Chim. Acta*, 1081 (2019) 51–58.
9. J. Zhou, Y. Zheng, J. Zhang, H. Karimi-Maleh, Y. Xu, Q. Zhou, L. Fu, W. Wu, *Anal. Lett.*, 53 (2020) 2517–2528.
10. D. Kipper, R.M. Hellfeldt, S. De Carli, F.K.M. Lehmann, A.S.K. Fonseca, N. Ikuta, V.R. Lunge, *Poult. Sci.*, 98 (2019) 5989–5998.
11. S.K. Pandey, A.C. Vinayaka, D.B. Rishi, P. Rishi, C.R. Suri, *Anal. Chim. Acta*, 841 (2014) 51–57.
12. N.J. Vickers, *Curr. Biol.*, 27 (2017) R713–R715.
13. G. Dai, Z. Li, F. Luo, S. Ai, B. Chen, Q. Wang, *Microchim. Acta*, 186 (2019) 1–9.
14. L. Wang, X. Huo, W. Qi, Z. Xia, Y. Li, J. Lin, *Talanta*, 211 (2020) 120715.
15. L. Fu, W. Su, F. Chen, S. Zhao, H. Zhang, H. Karimi-Maleh, A. Yu, J. Yu, C.-T. Lin, *Bioelectrochemistry* (2021) 107829.
16. M. Zhang, B. Pan, Y. Wang, X. Du, L. Fu, Y. Zheng, F. Chen, W. Wu, Q. Zhou, S. Ding, *ChemistrySelect*, 5 (2020) 5035–5040.
17. L. Fu, Q. Wang, M. Zhang, Y. Zheng, M. Wu, Z. Lan, J. Pu, H. Zhang, F. Chen, W. Su, *Front. Chem.*, 8 (2020) 92.
18. W. Li, W. Luo, M. Li, L. Chen, L. Chen, H. Guan, M. Yu, *Front. Chem.*, 9 (2021) 610.
19. H. Karimi-Maleh, A. Ayati, R. Davoodi, B. Tanhaei, F. Karimi, S. Malekmohammadi, Y. Orooji, L. Fu, M. Sillanpää, *J. Clean. Prod.*, 291 (2021) 125880.
20. H. Karimi-Maleh, F. Karimi, L. Fu, A.L. Sanati, M. Alizadeh, C. Karaman, Y. Orooji, *J. Hazard. Mater.*, 423 (2022) 127058.
21. Y. Zheng, J. Zhu, L. Fu, Q. Liu, *Int J Electrochem Sci*, 15 (2020) 9622–9630.

22. G. Liu, X. Yang, H. Zhang, L. Fu, *Int J Electrochem Sci*, 15 (2020) 5395–5403.
23. Y. Zheng, H. Zhang, L. Fu, *Inorg. Nano-Met. Chem.*, 48 (2018) 449–453.
24. H. Karimi-Maleh, F. Karimi, S. Malekmohammadi, N. Zakariae, R. Esmaeili, S. Rostamnia, M.L. Yola, N. Atar, S. Movaghgharnezhad, S. Rajendran, A. Razmjou, Y. Orooji, S. Agarwal, V.K. Gupta, *J. Mol. Liq.*, 310 (2020) 113185.
25. S. Yan, Y. Yue, L. Zeng, L. Su, M. Hao, W. Zhang, X. Wang, *Front. Chem.*, 9 (2021) 220.
26. S. Wei, X. Chen, X. Zhang, L. Chen, *Front. Chem.*, 9 (2021) 697.
27. L. Fu, A. Wang, G. Lai, W. Su, F. Malherbe, J. Yu, C.-T. Lin, A. Yu, *Talanta*, 180 (2018) 248–253.
28. X. Zhang, R. Yang, Z. Li, M. Zhang, Q. Wang, Y. Xu, L. Fu, J. Du, Y. Zheng, J. Zhu, *Rev. Mex. Ing. Quím.*, 19 (2020) 281–291.
29. J. Ying, Y. Zheng, H. Zhang, L. Fu, *Rev. Mex. Ing. Quím.*, 19 (2020) 585–592.
30. J. Lopez-Tellez, I. Sanchez-Ortega, C.T. Hornung-Leoni, E.M. Santos, J.M. Miranda, J.A. Rodriguez, *Chemosensors*, 8 (2020) 115.
31. L. Sørensen, L. Alban, B. Nielsen, J. Dahl, *Vet. Microbiol.*, 101 (2004) 131–141.
32. J. Hoorfar, D.L. Baggese, P. Porting, *J. Microbiol. Methods*, 35 (1999) 77–84.
33. R. Naravaneni, K. Jamil, *J. Med. Microbiol.*, 54 (2005) 51–54.
34. L. Lin, Q. Zheng, J. Lin, H.-G. Yuk, L. Guo, *Eur. Food Res. Technol.*, 246 (2020) 373–395.
35. L. Zhao, J. Wang, X.X. Sun, J. Wang, Z. Chen, X. Xu, M. Dong, Y. Guo, Y. Wang, P. Chen, *Front. Cell. Infect. Microbiol.*, 11 (2021) 60.
36. V. Pagliarini, D. Neagu, V. Scognamiglio, S. Pascale, G. Scordo, G. Volpe, E. Delibato, E. Pucci, A. Notargiacomo, M. Pea, *Electrocatalysis*, 10 (2019) 288–294.
37. L. Lou, P. Zhang, R. Piao, Y. Wang, *Front. Cell. Infect. Microbiol.*, 9 (2019) 270.
38. N.F. Silva, J.M. Magalhães, M.F. Barroso, T. Oliva-Teles, C. Freire, C. Delerue-Matos, *Talanta*, 194 (2019) 134–142.
39. J. Riu, B. Giussani, *TrAC Trends Anal. Chem.*, 126 (2020) 115863.
40. P. Pashazadeh, A. Mokhtarzadeh, M. Hasanzadeh, M. Hejazi, M. Hashemi, M. de la Guardia, *Biosens. Bioelectron.*, 87 (2017) 1050–1064.
41. N.F. Silva, J.M. Magalhães, M.F. Barroso, T. Oliva-Teles, C. Freire, C. Delerue-Matos, *Talanta*, 194 (2019) 134–142.
42. V.K. Rao, G. Rai, G. Agarwal, S. Suresh, *Anal. Chim. Acta*, 531 (2005) 173–177.
43. M.J. Allen, V.C. Tung, R.B. Kaner, *Chem. Rev.*, 110 (2010) 132–145.
44. W.S. Hummers Jr, R.E. Offeman, *J. Am. Chem. Soc.*, 80 (1958) 1339–1339.
45. D. Luo, G. Zhang, J. Liu, X. Sun, *J. Phys. Chem. C*, 115 (2011) 11327–11335.
46. R.R. Soares, R.G. Hjort, C.C. Pola, K. Parate, E.L. Reis, N.F. Soares, E.S. McLamore, J.C. Claussen, C.L. Gomes, *ACS Sens.*, 5 (2020) 1900–1911.
47. M.S. Awang, Y. Bustami, H.H. Hamzah, N.S. Zambry, M.A. Najib, M.F. Khalid, I. Aziah, A. Abd Manaf, *Biosensors*, 11 (2021) 346.
48. H. Sohrabi, M.R. Majidi, K. Asadpour-Zeynali, A. Khataee, A. Mokhtarzadeh, *Chemosphere* (2021) 132373.
49. H. Mohan, V. Ramalingam, J.-M. Lim, S.-W. Lee, J. Kim, J.-H. Lee, Y.-J. Park, K.-K. Seralathan, B.-T. Oh, *Colloids Surf. Physicochem. Eng. Asp.*, 607 (2020) 125469.
50. R. Silva-Leyton, R. Quijada, R. Bastías, N. Zamora, F. Olate-Moya, H. Palza, *Compos. Sci. Technol.*, 184 (2019) 107888.
51. I.A. Quintela, B.G. de Los Reyes, C.-S. Lin, V.C. Wu, *Front. Microbiol.*, 10 (2019) 1138.
52. W. Wei, J. Li, Z. Liu, Y. Deng, D. Chen, P. Gu, G. Wang, X. Fan, *J. Mater. Chem. B*, 8 (2020) 6069–6079.
53. M. Almas, U. Tahir, M. Zameer, M.I. Shafiq, S.Y. Farrukh, N. Zahra, M. Mazhar, S.A. Gill, F. Hadi, T. Muhammad, *J. Pharm. Res. Int.* (2021) 20–28.
54. L. Lu, Y. Ge, X. Wang, Z. Lu, T. Wang, H. Zhang, S. Du, *Sens. Actuators B Chem.*, 326 (2021)

- 128807.
55. Q. Chen, R. Gao, L. Jia, *Talanta*, 221 (2021) 121476.
 56. A.G. Mantzila, V. Maipa, M.I. Prodromidis, *Anal. Chem.*, 80 (2008) 1169–1175.
 57. B.-B. Wang, Q. Wang, Y.-G. Jin, M.-H. Ma, Z.-X. Cai, *J. Photochem. Photobiol. Chem.*, 299 (2015) 131–137.
 58. J. Dong, H. Zhao, M. Xu, Q. Ma, S. Ai, *Food Chem.*, 141 (2013) 1980–1986.
 59. A.S. Afonso, B. Pérez-López, R.C. Faria, L.H. Mattoso, M. Hernández-Herrero, A.X. Roig-Sagués, M. Maltez-da Costa, A. Merkoçi, *Biosens. Bioelectron.*, 40 (2013) 121–126.
 60. B. Shen, J. Li, W. Cheng, Y. Yan, R. Tang, Y. Li, H. Ju, S. Ding, *Microchim. Acta*, 182 (2015) 361–367.

© 2022 The Authors. Published by ESG (www.electrochemsci.org). This article is an open access article distributed under the terms and conditions of the Creative Commons Attribution license (<http://creativecommons.org/licenses/by/4.0/>).